national accelerator laboratory

EXP-41

April 4, 1973

ACCELERATOR EXPERIMENT--Mapping Stop Bands in the Main Ring at Injection

Experimentalists: R. Stiening, E.J.N. Wilson, D. Edwards

Date Performed: April 4, 1973

1. Motivation

The apparently small betatron amplitude which will survive in the main ring and the beam loss, both immediately after injection and during the parabola have puzzled operators and theorists alike for some time. The beam loss seems insensitive to closed orbit correction and to radial R.F. steering, yet the loss is precipitated by stimulating coherent betatron oscillations of only a few millimeters. We suspected that the loss might be to a virtual aperture stop, such as the unstable region which lies outside the separatix of a resonance, rather than to a physical obstacle. We, therefore, set out to explore the mesh of resonance stop bands in the working space:

$$20 < \nu x,\ \nu y < 20 \cdot 5$$

Theory predicts that third and fourth order stop bands may be driven by sextupole or octupole errors in the main ring magnets. The errors might be fluctuations in the strong remanent sextupole field known to exist in both B1 and B2 or to geometrical errors in magnet assembly. These errors have a random

distribution which can contain the appropriate Fourier component to drive the resonance, e.g. 61st harmonic drives $\nu = 20 \cdot 33$.

2. Technique

The experiments at 8 GeV were performed using the prepulse with R.F. on and with constant field. A single radial or vertical position monitor signal (VF45 or HF46) was displayed and photographed from a CRT together with a circulating beam signal. (Figure 1) Beam survival over the first 0.4 seconds after injection was measured from the intensity trace. The position monitor trace was triggered at 0.4 seconds at the instant that a pinger was fired to excite coherent betatron oscillations in the beam. From the frequency of these oscillations the tune of the surviving beam was measured.

The tune of the machine was adjusted with the Q Bump (average quadrupole current) together with the tune splitter which alters the current in the D quads. The perturbations were programmed to occur only during the prepulse. Once a correlation between the preturbations and the tune measurements had been established, we deduced the tune from the currents. This was necessary because near a stop band, betatron oscillations either lock on to the beam as it is extracted or indicate the tune of the small and non-representative population of protons which stay in the machine.

3. Results

a. Scan along $\nu x = \nu y$

After a first exploratory traverse along the diagonal $\nu x = \nu y$, a scan at intervals of 0.01 in tune was made. One photograph was taken at each

point. (Figure 2) The influence of all the stop bands up to fourth order can be clearly seen. The one third seemed particularly wide, as did the superposition of all orders of stop band at the integer. Between these two regions there was no clear plateau where survival approached 100%. We interpret this as an indication that the third and perhaps the fourth integer stop bands merge into a continuum for protons of largish amplitude and combine to eject the periphery of the injected beam. The strength of the third integer stop band varies linearly with amplitude, the quarter integer increases quadratically. Since the beam is 1 cm diameter at half height, this represents a formidable limitation on the performance of the machine which must be overcome before larger beams from the booster can be accelerated. This aperture limitation causes the initial loss which can be clearly seen on the intensity trace. (Figure 1) It is followed by an exponential decay stretching right out to 0.4 seconds. We think this is due to gas scattering which will cause the beam to grow in betatron amplitude and leak out into the unstable region. Both the initial loss and the slow exponential become more marked as the machine is tuned close to stop bands and eventually no beam survives. The resonant process is similar to that employed in slow resonant extraction.

The rounding of the peaks in Figure 2 can be due to the tune spread in the beam due to momentum spread. Although $d\nu_y/dp$ had been very well compensated, $d\nu_x/dp$ cannot yet be independently varied, it was measured to be 20 during the run. This, for a momentum spread of $\pm 0.1\%$, would produce a tune

spread of 0·04. Another potential source of tune spread (the amplitude dependence due to zero harmonic octupole errors) proved to be very small at these amplitudes and was further reduced by setting the 48 correction octupoles to 15 amps/magnet.

b. Compensation of a Stop Band

Until further correction magnets are installed we are somewhat limited in the correction we can apply. Nevertheless, a sine and cosine phase of 61st harmonic sextupole can be generated and was used to cancel out one of the four intersecting third order resonance, $3\nu x = 61$. To do this we placed the working point at the resonant value and varied the two phases of the harmonic. The contour plot of the transmission is to be seen in Figure 3. The width of the $\nu x = 20\cdot\dot{3}\dot{3}$ stop band can be deduced from the amplitude of this correction. The full width is found to be within 0·02 and 0·03 for a beam of this size. This is also not inconsistent with what is known about the strength of remanent sextupole field in B1's and B2's. The wide valleys in Figure 2 seem about twice as wide as this, perhaps because several stop bands combine on the diagonal. The width of the quarter integer checks well with what is known about the octupole content of the remanent field in the quadrupoles.

A second scan with the sextupoles at their best setting revealed an improved transmission on either side of the 20 1/3 complex of resonances. (Figure 4) We extended this scan to cross the half integer. Clearly one cannot expect a marked improvement until further multipoles are installed to attack the other resonances at the $20\cdot\dot{3}\dot{3}$ value.

c. Survey of the Diamond

With the aid of the tune splitter we were able to make similar scans along lines parallel to the main diagonal but displaced to have tune splits of ±0·06, ±0·12, ±0·18, ±0·25. Figure 5 shows the survival plotted as a contour map. The two islands of stability are to be seen and a vestige of survival with a large tune split. The pattern of known stop bands fits the contour map well.

Clearly the normal operating point is correctly centered in the largest region of stability at $\nu x = \nu y = 20 \cdot 2$.

d. Measurements at 27 GeV

If the stop bands are excited by the remanent field pattern rather than by geometrical errors in magnet assembly, the stop bands should be much narrower at 27 GeV.

We repeated the 8 GeV diagonal scan on a 27 GeV flat top. The conditions were somewhat different. The initial fast loss could not be included in the survival ratio calculation. Survival was measured not at 0·6 sec but over a 1·5 sec interval on the flat top. These two effects might be expected to compensate to some extent.

The other difference was that measurements clearly showed that νx and νy were split by 0·05. This should reduce the clear space between resonances. We did not employ the tune splitter to correct for this split.

Figure 6 shows the survival scan. Loss at the peak is smaller than at 8 GeV but it is difficult to say whether the resonances have become narrower.

At 27 GeV the momentum spread will be larger than at injection due to the recent passage through transition and a measurement of the chromaticity at 27 GeV revealed a $d\nu_x/dp$ of 30. It is possible that the apparent width of the resonances at 27 GeV is broadened somewhat by the chromaticity. The width of the third is certainly broadened by the staggering of $_\nu x$ and $_\nu y$.

This particular experiment must be repeated at a higher energy and using a programmed tune split to restore to the diagonal before one can identify the origin, remanent or geometrical, of the errors which will have to be compensated.

4. Future Work

Clearly a powerful diagnostic method is now available and we intend to use it to try to compensate stop bands once the necessary correction magnets become available. Independent control of vertical and radial chromaticities may also aid beam survival but to enlarge the 1 cm "hole" within the stop bands in order to accept a larger booster beam may take some time even if the compensation proves only to be necessary at injection.

Should the driving errors prove to be geometrical in origin rather than remanent, ramped corrections will have to be applied at least up to 50 GeV. Setting up this kind of energy dependent correction may prove a very long business. We, therefore, wish to identify the source of the errors as quickly as we can.

It still remains a possibility that the resonances, which seem somewhat broader than theory would predict from the remanent field, are driven by a few

bad magnets or by the stray field of a beam transfer magnet. The search for such objects should not be abandoned.

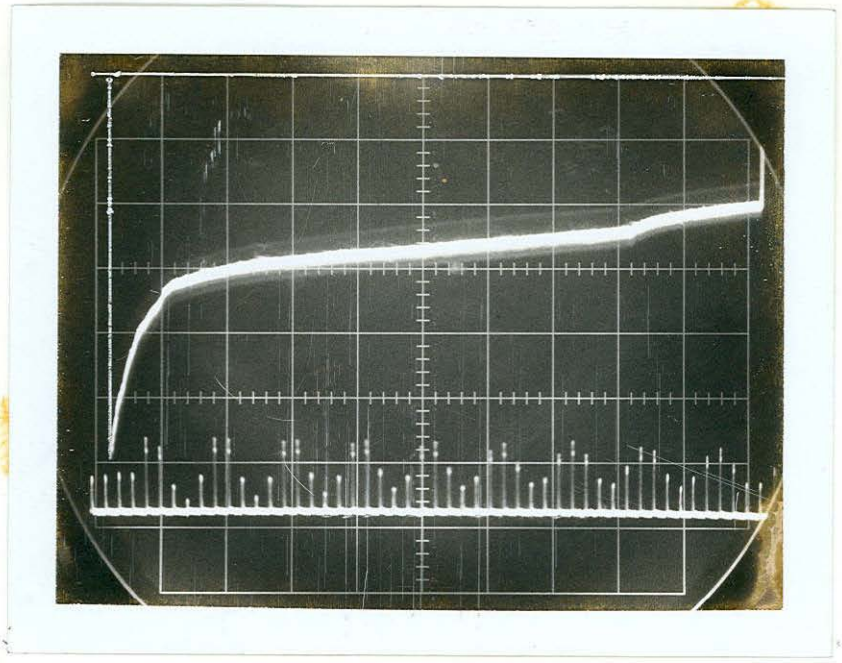

UPPER TRACE: CIRCULATING BEAM (INVERTED)
100 ms./div.

LOWER TRACE: RADIAL POSITION SHOWING
COHERENT OSCILLATION
AFTER PING
100 ms./div.

FIGURE 1

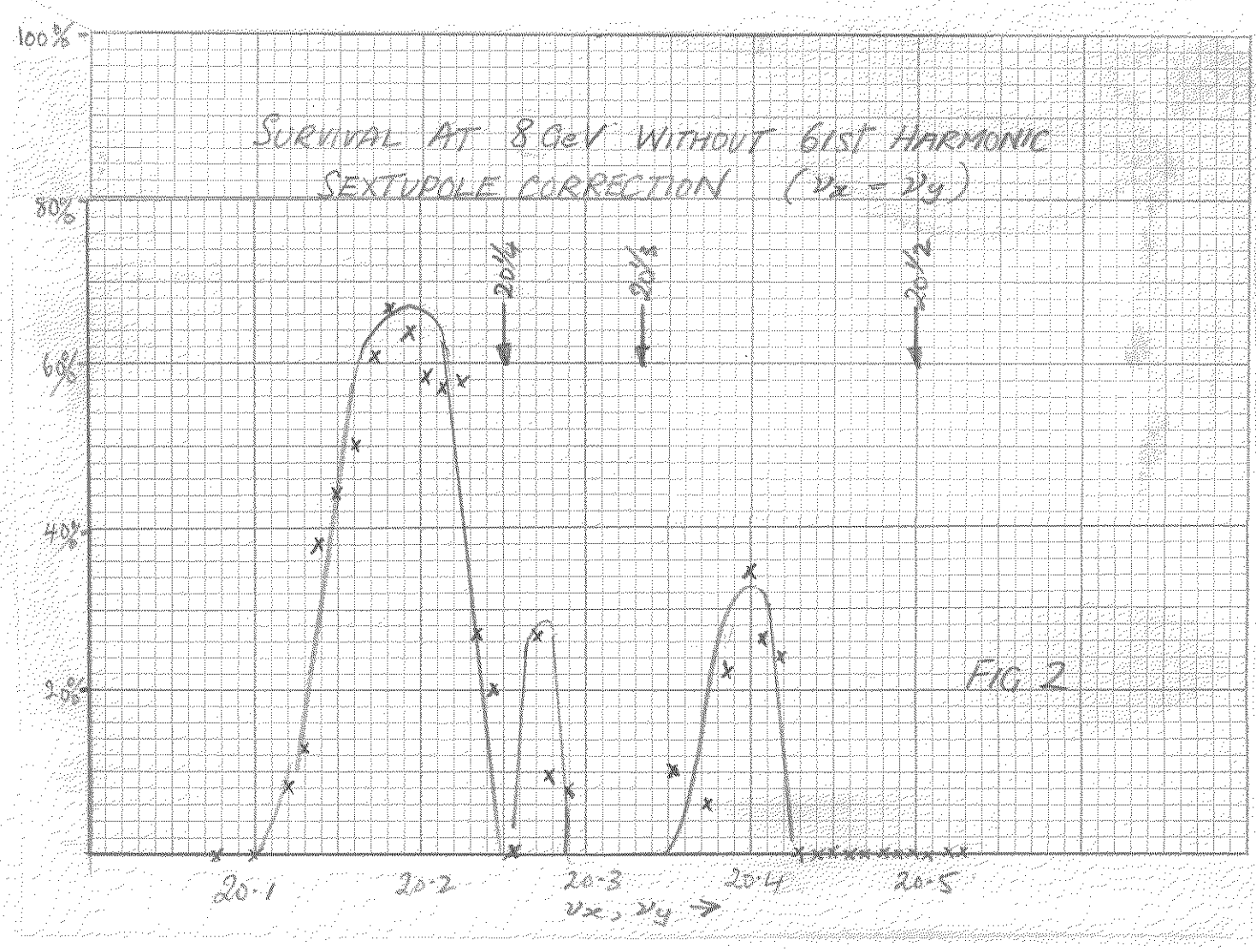
SURVIVAL AT 8 GeV WITHOUT 61ST HARMONIC SEXTUPOLE CORRECTION ($\nu_x - \nu_y$)
100%
80%
60%
40%
20%
20·1
20·2
20·3
20·4
20·5
ν_x, ν_y →
FIG 2

FIGURE 2

K&E 20 X 20 TO THE INCH 46 1240
7 X 10 INCHES MADE IN U.S.A.
KEUFFEL & ESSER CO.

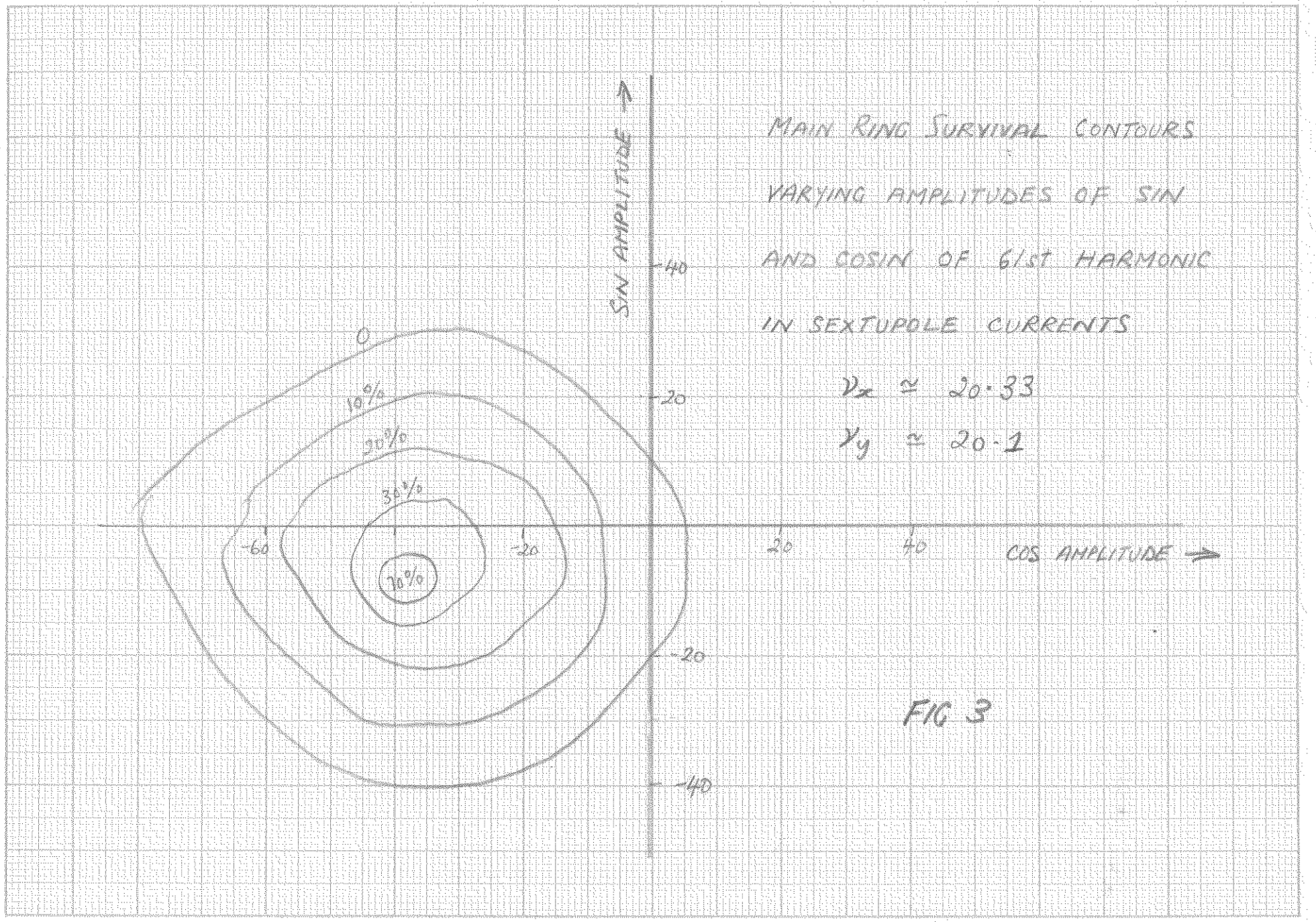

FIGURE 3

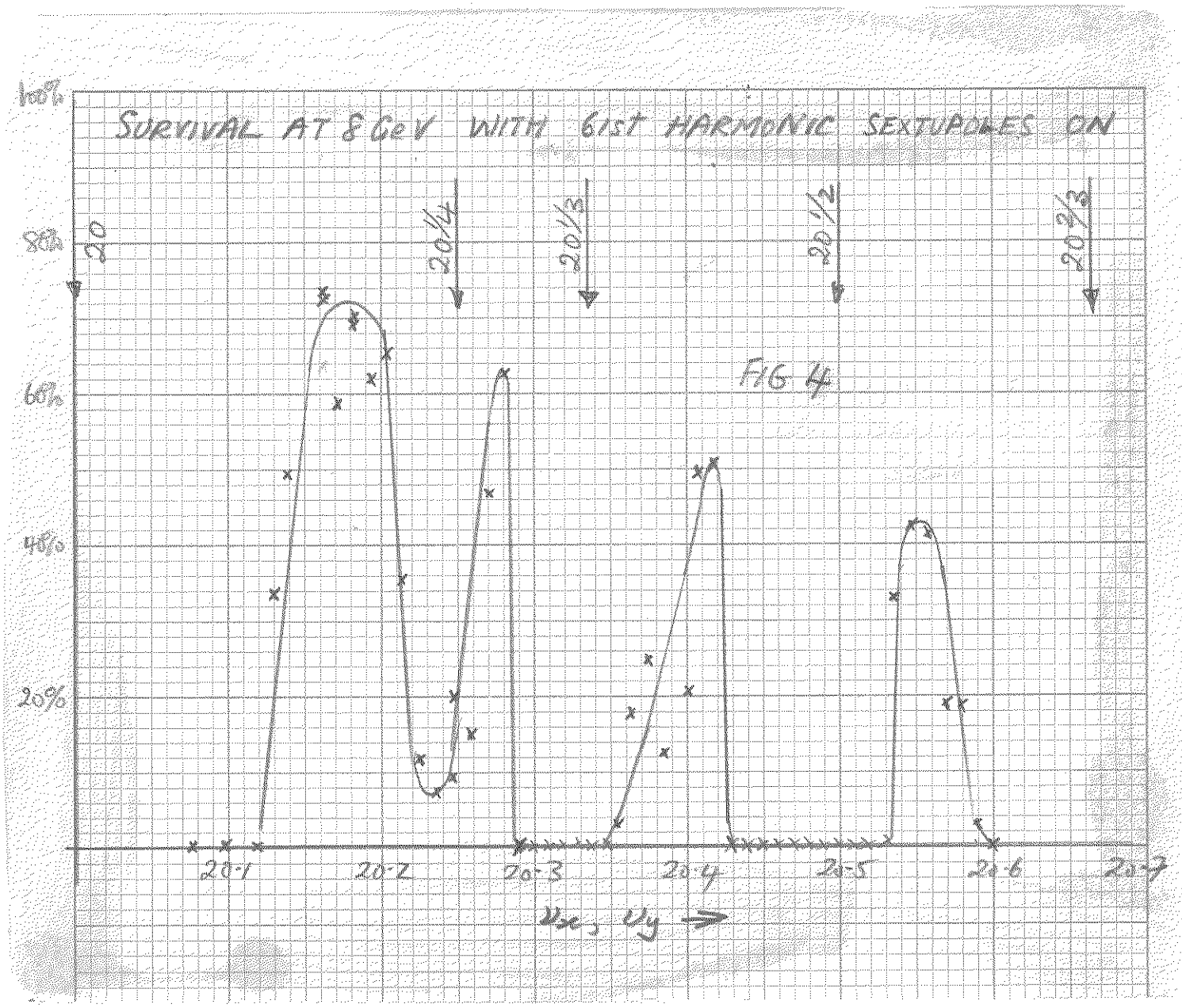
SURVIVAL AT 8 GeV WITH 61ST HARMONIC SEXTUPOLES ON
100%
80%
60%
40%
20%
20
20 1/4
20 1/3
20 1/2
20 2/3
FIG 4
20-1
20-2
20-3
20-4
20-5
20-6
20-7
νx, νy

FIGURE 4

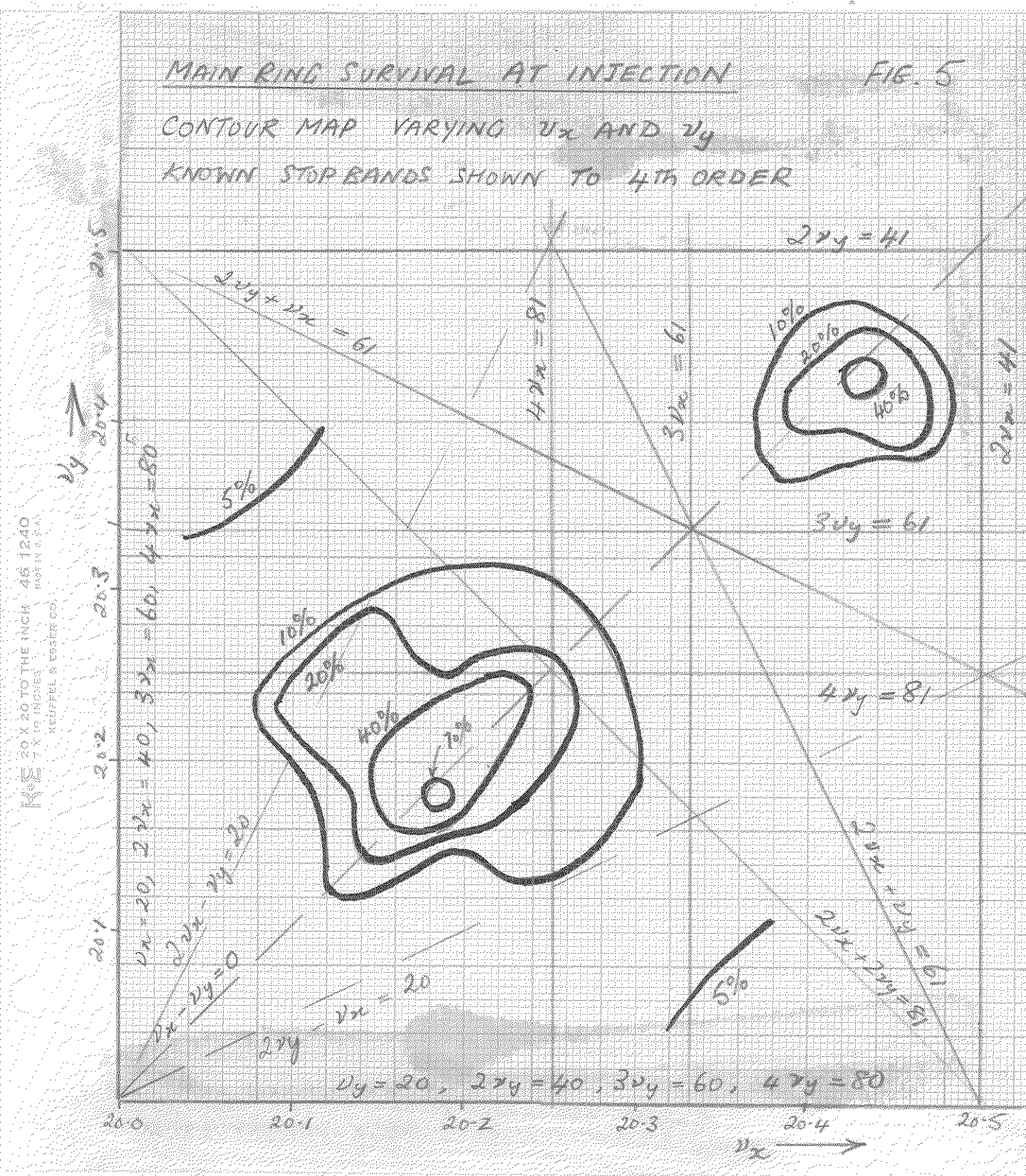
MAIN RING SURVIVAL AT INJECTION
FIG. 5
CONTOUR MAP VARYING ν_x AND ν_y
KNOWN STOPBANDS SHOWN TO 4TH ORDER
$2\nu_y = 41$
$2\nu_x = 41$
$3\nu_y = 61$
$4\nu_y = 81$
$\nu_x + 2\nu_y = 61$
$2\nu_x + \nu_y = 61$
$3\nu_x = 61$
$4\nu_x = 81$
$2\nu_x - 2\nu_y = 0$
$\nu_x - \nu_y = 0$
$\nu_x = 20$
$2\nu_y$
$\nu_y = 20,\ 2\nu_y = 40,\ 3\nu_y = 60,\ 4\nu_y = 80$
ν_y
ν_x
20·0
20·1
20·2
20·3
20·4
20·5
10%
20%
40%
5%

FIGURE 5

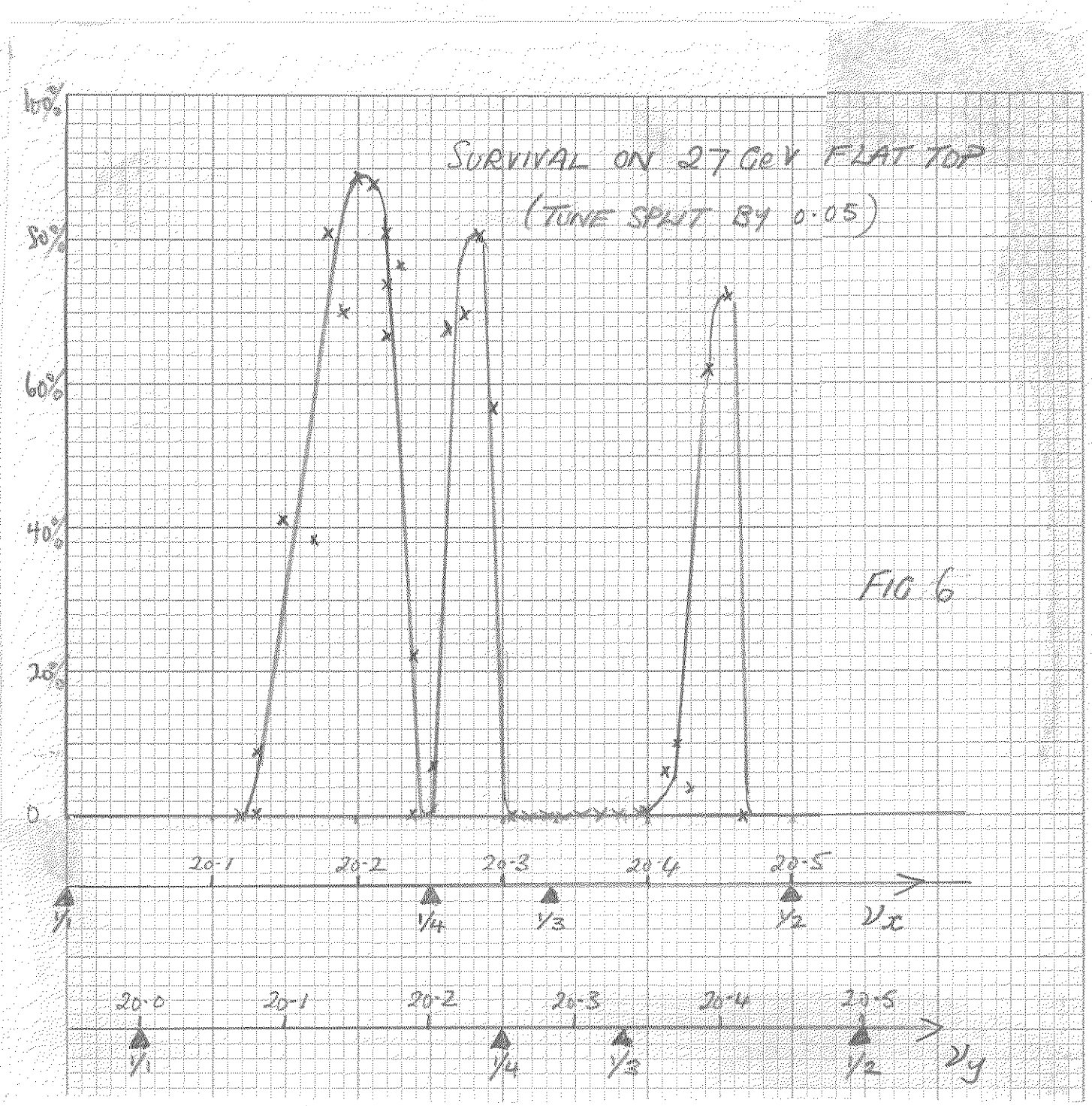
SURVIVAL ON 27 GeV FLAT TOP
(TUNE SPLIT BY 0.05)
100%
80%
60%
40%
20%
0
20.1
20.2
20.3
20.4
20.5
1/4
1/3
1/2
ν_x
20.0
20.1
20.2
20.3
20.4
20.5
1/4
1/3
1/2
ν_y
FIG 6

FIGURE 6